

Mean escape depth of signal photoelectrons ejected from solids by polarized x rays

I. S. Tilinin

*Department of Applied Surface Science, Institute of Physical Chemistry, Polish Academy of Sciences, ul. Kasprzaka 44/52,
01-224 Warsaw, Poland*

(Received 05 June 1995)

Quick development of synchrotron radiation facilities and prospective applications of photon beams of a variable energy in spectroscopy of solids and interfaces prompts further studies of photoemission induced by polarized soft x rays. One of the most important characteristics in surface sensitive spectroscopies is the mean escape depth of signal electrons leaving a sample without being scattered inelastically. In this article a simple analytical expression for the average escape depth of photoelectrons ejected by polarized x rays is found by means of the depth distribution function obtained by solving the transport equation. The dependence of the escape depth on the type and the degree of photon polarization is predicted. This effect is due to the anisotropy of the initial angular distribution of photoelectrons and elastic scattering they suffer on their way out of the target. The variation of the mean escape depth with the type and the degree of polarization as well as with the emission direction from the target is quite well pronounced and may reach up to 100% with respect to the value determined by the inelastic mean free path in the usual x-ray photoelectron spectroscopy formalism. The dependence of the escape depth on the azimuthal and polar emission angles is studied in detail. In the special case of unpolarized x rays the expression for the average escape depth reduces to the result found earlier.

I. INTRODUCTION

The widely used surface sensitive techniques such as Auger (AES) and x-ray photoelectron (XPS) spectroscopies are based on measuring energy distributions of secondary electrons in the vicinity of the characteristic peaks corresponding to signal electrons carrying direct information about the elemental composition of top monolayers. The majority quantity characterizing the surface sensitivity is the mean escape depth D defined as the average emission depth pertaining to the depth distribution function in the problem considered.^{1,2} The depth distribution function describes the probability for an electron generated at a certain depth to be emitted from a sample in a certain direction. In the usual AES/XPS formalism it has been believed that elastic scattering of signal electrons on their way out of the target can be neglected and that the escape probability obeys a simple exponential law.³ Under this assumption the mean escape depth is determined by a simple product of the inelastic mean free path λ_i and the cosine of the emission angle α , $D = \lambda_i \cos \alpha$. Recent studies⁴⁻⁶ indicate, however, that elastic scattering may significantly modify the quantity D and thereby influence the surface sensitivity. It was found, in particular, that the mean escape depth of photoelectrons ejected from solids by unpolarized radiation is strongly anisotropic even in the case of amorphous or polycrystalline targets where no noticeable dynamical diffraction effects are expected.^{4,5} The latter effect is due to a mutual interference of anisotropy of the differential atomic photoelectric cross section and photoelectron elastic collisions.

Meanwhile rapid development of synchrotron radiation facilities makes possible the usage of polarized x rays in surface analysis.^{7,8} Especially promising in this respect is the scanning XPS as a nondestructive method for three-dimensional microprobing.^{9,10} In this connection the generalization of the results found in Ref. 4 for unpolarized radia-

tion to the case of polarized x rays seems highly desirable.

In the present article the analytical expression for the mean escape depth of signal photoelectrons emitted from a sample irradiated by polarized x rays has been derived on the basis of the kinetic equation approach. An effect—the dependence of the mean escape depth on the type and the degree of polarization of incident photons—is predicted and analyzed in detail. Such an optical orientation transfer to the escape probability seems to have few analogies in literature.

II. PHOTON POLARIZATION AND INITIAL ANGULAR DISTRIBUTION OF PHOTOELECTRONS

Consider a broad beam of x rays incident at the angle ϑ , at a flat semi-infinite target. We choose the coordinate system with the Z axis directed towards the bulk of the target and the XY plane coinciding with the surface. The X axis is assumed to be parallel while the Y axis is normal to the plane of incidence containing the x-ray propagation direction and the surface normal (see Fig. 1). In addition, we introduce a rotated coordinate system xyz with the z axis along the photon propagation direction and the y axis coinciding with the Y axis of the laboratory system XYZ . To characterize the polarization state of incident photons we also introduce a degree of polarization p and the unit polarization vector

$$\hat{\epsilon} = e^+ \exp(-i\gamma) \cos\left(\eta - \frac{1}{4}\pi\right) + e^- \exp(i\gamma) \sin\left(\eta - \frac{1}{4}\pi\right), \quad (1)$$

where e^\pm are the unit vectors in the coordinate system xyz and pertain to the positive and negative helicity states, respectively.¹¹ The polarization vector being equal to e^\pm is interpreted as a right (+) or left (−) circular polarization. Thus expression (1) represents the expansion of the polarization vector in the complete basis $\{e^+, e^-\}$. The parameters η and γ specify the type and the azimuthal orientation of po-

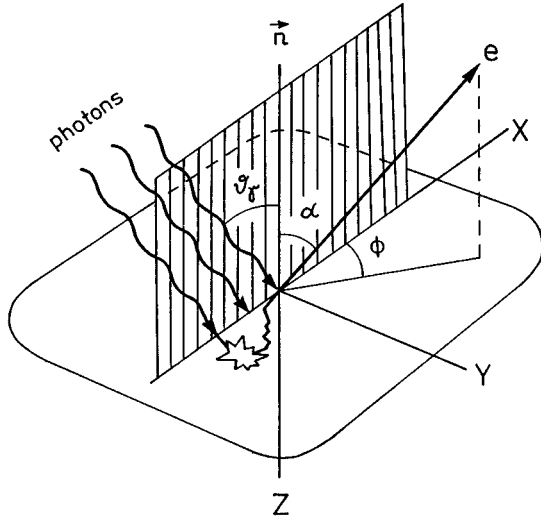


FIG. 1. Schematic representation of the typical XPS geometrical configuration. A beam of x rays is incident at the polar angle ϑ_γ on a target. The photoelectron emission direction is described by the polar angle α and the azimuthal angle ϕ .

larization and vary from $-\pi/2$ to $+\pi/2$ and from 0 to π , respectively. Namely, in the general case of the elliptical polarization, the quantity γ equals the angle the principal axis of the polarization ellipse is rotated by, with respect to the x axis. The parameter η determines the amounts of right and left circular polarization in a pure polarization state. In particular, the case $\eta=0$ corresponds to the linear polarization when the amplitude of the electric-field vector is at the angle γ to the x axis. Similarly, $\eta=\pm\pi/2$ denotes the linear polarization with the electric-field amplitude oriented along the direction making the angle γ (+) or $\pi-\gamma$ (-) with the y axis. The electric-field vector precesses according to the sign of the parameter η . The positive values of $\eta>0$ correspond to the anticlockwise rotation, while the negative ones correspond to the clockwise precession of the electric field. The most general polarization state can be regarded as a mixture of completely polarized and unpolarized states and is described by the density matrix^{11,12}

$$\rho = \frac{1}{2} \begin{pmatrix} 1+p \sin 2\eta & -p \exp(-2i\gamma) \cos 2\eta \\ -p \exp(2i\gamma) \cos 2\eta & 1-p \sin 2\eta \end{pmatrix}. \quad (2)$$

Note that in the case $p=1$ density matrix (2) describes a completely polarized photon beam.

The initial angular distribution of photoelectrons is determined by the differential photoelectric cross section which in the coordinate system xyz is given by¹¹

$$d\sigma_{\text{ph}}/d\Omega = \sigma_{\text{ph}} f(\Theta, \Phi), \quad (3)$$

$$f(\Theta, \Phi) = (1/4\pi) \{ 1 - (\beta/2) [P_2(\cos\Theta) + (3/2) \times (S_1 \cos 2\Phi + S_2 \sin 2\Phi) \sin^2\Theta] \}, \quad (4)$$

where σ_{ph} is the total photoelectric cross section, β is the asymmetry parameter, $P_2(x)$ is the Legendre polynomial of the second order, Θ and Φ are the polar and azimuthal angles

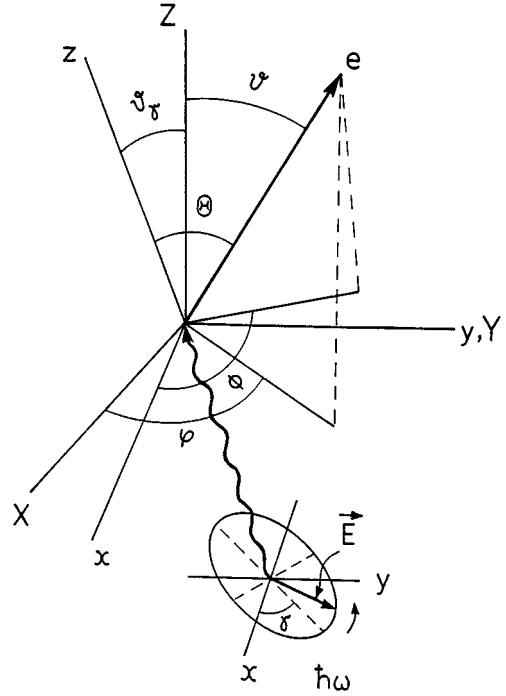


FIG. 2. Disposition of the coordinate systems xyz and XYZ used in angular distribution formulas. Also shown is the polarization ellipse rotated at the angle γ with respect to the x axis in the xy plane. The electric-field vector E precesses anticlockwise (right polarization).

specifying the photoelectron momentum in the system of coordinates xyz (see Fig. 2), while S_1 and S_2 are the Stokes parameters¹³⁻¹⁵

$$S_1 = -p \cos 2\eta \cos 2\gamma, \quad (5)$$

$$S_2 = -p \cos 2\eta \sin 2\gamma. \quad (6)$$

For further consideration it is advisable to rewrite the differential photoelectric cross section in terms of the polar angle ϑ and the azimuthal angle φ describing the photoelectron direction of motion in the system of coordinates XYZ . This is achieved by replacing the normalized differential photoelectric cross section $f(\Theta, \Phi)$ in formula (3) by the function $f(\vartheta, \varphi)$ of the form

$$f(\vartheta, \varphi) = (1/4\pi) \{ 1 - (\beta/4) [3\zeta_0(\vartheta, \varphi) + 3S_1\zeta_1(\vartheta, \varphi) + 3S_2\zeta_2(\vartheta, \varphi) - 1] \}. \quad (7)$$

In the latter expression the functions $\zeta_i(\vartheta, \varphi)$ ($i=0,1,2$) are defined by the relationships

$$\zeta_0(\vartheta, \varphi) = (\cos\vartheta_\gamma \cos\vartheta + \sin\vartheta_\gamma \sin\vartheta \cos\varphi)^2, \quad (8)$$

$$\zeta_1(\vartheta, \varphi) = \cos^2\vartheta_\gamma \sin^2\vartheta \cos 2\varphi - \cos\vartheta_\gamma \sin\vartheta_\gamma \sin 2\vartheta \cos\varphi + \sin^2\vartheta_\gamma (\cos^2\vartheta - \sin^2\vartheta \sin^2\varphi), \quad (9)$$

$$\zeta_2(\vartheta, \varphi) = \cos\vartheta_\gamma \sin^2\vartheta \sin 2\varphi - \sin\vartheta_\gamma \sin 2\vartheta \sin\varphi. \quad (10)$$

Formula (7) follows immediately from expression (4) if one takes into account that the coordinate system xyz is obtained from the system XYZ by a rotation with the Euler angles $(0, \vartheta_\gamma, 0)$. In the case of unpolarized radiation ($p=0$) formula (7) reduces to the well-known result of Reilman.¹⁶

Since the transport mean free path and the attenuation length of x rays are large compared with the effective escape depth of signal photoelectrons the photoelectron source function Q may be considered as independent of depth. Thus, we have for the initial distribution of electrons in the target

$$Q(\Omega_0) = MF\sigma_{\text{ph}}f(\Omega_0, \Omega_\gamma), \quad (11)$$

where M is the atomic bulk density and F is the initial flux of incident photons, the unit vectors $\Omega_0 = \Omega_0(\vartheta, \varphi)$ and $\Omega_\gamma = \Omega_\gamma(\vartheta_\gamma, 0)$ refer to the photoelectron initial direction of motion and that of x-ray propagation.

III. SOLUTION OF TRANSPORT PROBLEM

Calculation of the mean escape depth of photoelectrons requires knowledge of the escape probability as a function of depth of origin $\Phi(z, \Omega)$ (here z is the emission depth and the vector Ω characterizes the direction at which a photoelectron leaves a target). This function is often referred to as the depth distribution function (DDF).¹ The DDF is shown to be proportional to the outgoing flux density of particles times the cosine of the emission angle.¹⁷ Thus, to find the DDF it is necessary to solve a transport equation with a source function corresponding to a point source of electrons located at a certain depth z . The obtained solution is to satisfy the boundary condition implying that no secondary electrons enter the sample.

The boundary-value problem involving a linearized Boltzmann-type kinetic equation can be solved most effectively in the transport approximation^{4,17} under the condition that the angular distribution of particles is a slowly varying function of emission angles.¹⁸ This requirement is perfectly met in the case of Auger and photoelectron emission [cf. formula (7)]. In the transport approximation the exact differential elastic-scattering cross section in the collision integral is replaced by an isotropic one equal to the corresponding momentum transfer (or transport) cross section. Therefore, in this approach, the only quantities characterizing electron-solid interaction are the inelastic (λ_i) and the transport (λ_{tr}) mean free paths. Such a replacement is justified by fundamental properties of the transport equation. Namely, this approximation satisfies the so-called generalized radiative field similarity principle^{18,19} and provides similarity between the exact and the approximate solutions in the limiting cases of weak ($\lambda_i \gg \lambda_{\text{tr}}$) and strong ($\lambda_i \leq \lambda_{\text{tr}}$) absorption.

The accuracy of the transport approximation has been checked recently by comparison with Monte Carlo simulation results based on a realistic Mott differential elastic-scattering cross section.^{4,17-22} It was found that the transport

approximation predictions for different emission characteristics were astonishingly accurate, even in the intermediate case of scattering parameters, $\lambda_i \sim \lambda_{\text{tr}}$, which is of the most relevance for XPS. The discrepancies between the Monte Carlo and analytical results, as a rule, do not exceed several percent as regards the angular and energy spectrum of emitted electrons,^{19,20} the emission depth and the traveled path-length distributions,^{17,21} the mean escape depth,⁴ the total photoelectron yield,²² and so on. In view of this it seems appropriate to apply the transport approximation to the problem of signal photoelectron emission by polarized x rays.

For the sake of brevity we do not present a mathematical formulation of the secondary emission problem in full. This formulation is discussed in detail in recent publications.^{4,18-22} The depth distribution function $\Phi(\Omega, z)$ can be expressed through the surface value of the Green's function of the transport equation

$$\Phi(\Omega, z) = \mu y_0 \int G(0, \Omega | z, \Omega_0) f(\Omega_0, \Omega_\gamma) d\Omega_0. \quad (12)$$

Here $\Omega = \Omega(\alpha, \phi)$ is the unit vector along the emission direction from the solid,

$$y_0 = MF\sigma_{\text{ph}} \quad (13)$$

is the normalization prefactor, and $\mu = \cos \alpha$ is the cosine of the emission polar angle (see Fig. 1). In the transport approximation the Green's function $G(z, \Omega | z_0, \Omega_0)$ obeys the equation

$$\xi \frac{\partial G}{\partial \tau} = -G + \frac{1}{4\pi} \int G(\tau, \Omega' | \tau_0, \Omega_0) d\Omega' + \delta(\Omega - \Omega_0) \quad (14)$$

with the boundary condition

$$G(0, \Omega | \tau_0, \Omega_0) = 0, \quad \text{for } \xi = (e_z \cdot \Omega) > 0, \quad (15)$$

where e_z is the unit vector along the Z axis, τ is the dimensionless depth

$$\tau = z/\lambda, \quad (16)$$

and λ is the total mean free path in the transport approximation

$$\lambda = \lambda_i \lambda_{\text{tr}} (\lambda_i + \lambda_{\text{tr}})^{-1}. \quad (17)$$

The solution to Eq. (14) with boundary condition (15) can be found by Case's method of eigenfunctions.²³ Particularly, the surface value of the Green's function reads²⁴

$$\begin{aligned} G(0, \Omega | \tau, \Omega_0) = & (2\pi)^{-1} \left(H(\mu, \omega) (\omega \nu_0 (\nu_0^2 - 1)) \{ 2(\nu_0 - \mu)(\nu_0 - \mu_0) [1 + \nu_0^2(\omega - 1)] H(\nu_0, \omega) \}^{-1} \exp(-\tau/\nu_0) \right. \\ & + \int_0^1 \varphi_\nu(\mu) \varphi_\nu(\mu_0) g(\nu, \omega) [\nu H(\nu, \omega)]^{-1} \exp(-\tau/\nu) d\nu - \mu^{-1} \cdot \delta(\mu - \mu_0) \exp(-\tau/\mu) \Big) \\ & + \mu^{-1} \cdot \delta(\Omega - \Omega_0) \exp(-\tau/\mu). \end{aligned} \quad (18)$$

In formula (18) ω is the single scattering albedo

$$\omega = \lambda/\lambda_{tr}. \quad (19)$$

$H(\mu, \omega)$ is the H function of Chandrasekhar²⁵ for an isotropically scattering medium, $\varphi_\nu(\mu)$ is the eigenfunction of the homogeneous transport equation pertaining to the continuous eigenvalue set $0 \leq \nu \leq 1$,^{17,23} the quantity ν_0 is the root of the characteristic equation

$$1 = (\omega \nu_0/2) \cdot \ln[(\nu_0 + 1)/(\nu_0 - 1)], \quad (20)$$

and the function $g(\nu, \omega)$ is given by the expression

$$g(\nu, \omega) = \{(\pi \omega \nu/2)^2 + [1 - (\omega \nu/2) \cdot \ln[(1 + \nu)/(1 - \nu)]]^2\}^{-1}. \quad (21)$$

Expressions (12) and (18) along with the source function defined by Eqs. (7) and (11) determine completely the escape probability as a function of the depth of origin.

IV. MEAN ESCAPE DEPTH

The mean escape depth D can be calculated by means of the formula

$$D = \lambda \left(\int_0^\infty \tau \Phi(\tau, \Omega) d\tau \right) \left(\int_0^\infty \Phi(\tau, \Omega) d\tau \right)^{-1}, \quad (22)$$

where the depth distribution function Φ is conveniently expressed in terms of the reduced depth τ . Substitution of the explicit expression for the DDF into the right-hand side of Eq. (22) yields the ratio of two multiple integrals. The integration is performed over all photoelectron emission depths and initial directions of motion. In addition there are integrals over the eigenvalues of the continuum set. The integration over τ does not pose any problem as it follows from formula (18). Calculation of the integrals over ν can be carried out by means of the residue theorem.⁶ Making use of identities involving the H function of Chandrasekhar²⁵ it is possible to present the final expression for the mean escape depth in the form

$$D = \frac{\lambda_i \lambda_{tr}}{\lambda_i + \lambda_{tr}} (\cos \alpha + W). \quad (23)$$

Here the quantity W depends on the geometrical configuration and scattering properties of the target. It is defined by the ratio

$$W = W_1/W_2 \quad (24)$$

so that

$$W_1 = (1 - \omega)^{-1/2} \chi - V_1, \quad (25)$$

$$W_2 = (1 - \omega)^{-1/2} - \frac{\beta}{4H(\cos \alpha, \omega)} \times [3 \cos^2 \psi - 1 + 3S_1 \zeta_1(\alpha, \phi) + 3S_2 \zeta_2(\alpha, \phi)] + V_2. \quad (26)$$

In formulas (25) and (26) ψ is the angle between the photon propagation direction and that of the photoelectron emission, while χ , V_1 and V_2 are the integrals given by the expressions

$$\chi = (\omega/2)(1 - \omega)^{-1/2} \int_0^1 \mu H(\mu, \omega) d\mu, \quad (27)$$

$$V_1 = \frac{\omega \beta}{16} [3\mu_\gamma^2 - 1 + 3S_1(1 - \mu_\gamma^2)] \times \int_0^1 \frac{(x^2 + x \cos \alpha) H(x, \omega) (3x^2 - 1) dx}{(x + \cos \alpha)}, \quad (28)$$

$$V_2 = \frac{\omega \beta}{16} [3\mu_\gamma^2 - 1 + 3S_1(1 - \mu_\gamma^2)] \int_0^1 \frac{x H(x, \omega) (3x^2 - 1) dx}{(x + \cos \alpha)}. \quad (29)$$

When deriving expressions (25) and (26) and (28) and (29) we set $\mu_\gamma = \cos \vartheta_\gamma$ and made the interchange

$$\vartheta = \pi - \alpha, \quad \xi = -\cos \alpha. \quad (30)$$

In accordance with (30) the functions $\zeta_1(\alpha, \phi)$ and $\zeta_2(\alpha, \phi)$ read

$$\zeta_1(\alpha, \phi) = \cos^2 \vartheta_\gamma \sin^2 \alpha \cos 2\phi + \cos \vartheta_\gamma \sin \vartheta_\gamma \sin 2\alpha \cos \phi + \sin^2 \vartheta_\gamma (\cos^2 \alpha - \sin^2 \alpha \cos^2 \phi) \quad (31)$$

$$\zeta_2(\alpha, \phi) = \cos \vartheta_\gamma \sin^2 \alpha \sin 2\phi + \sin \vartheta_\gamma \sin 2\alpha \sin \phi. \quad (32)$$

In the limiting case of weak scattering ($\lambda_{tr} \rightarrow \infty$) single scattering albedo ω tends to zero and the quantity W_1 becomes small compared with W_2 . Thus, in the absence of elastic-scattering formula (23) reduces to the well-known result of the usual XPS formalism, $D = \lambda_i \cos \alpha$. The opposite limiting case ($\lambda_{tr} \ll \lambda_i$) corresponds to intensive elastic scattering against the background of weak absorption. The leading term in the round brackets of the right-hand side of expression (23) becomes proportional to the square root of the ratio $\lambda_i/\lambda_{tr} \gg 1$. As a result the mean escape depth is almost independent of the emission direction, $D \sim (\lambda_i \lambda_{tr})^{1/2}$. Hence we see that in the case of intensive scattering the escape depth is determined by the average displacement from the point of origin or by the diffusion length. That obviously corresponds to a diffusionlike picture of the particle transport.

In practical XPS applications, however, the most important is the situation when the inelastic mean free path is of the order of the transport mean free path, $\lambda_i \sim \lambda_{tr}$. In the latter case the quantity D is a complicated function of the photoelectron emission direction, the type and degree of incident photon polarization. Deviations of the mean escape depth from the simple result of the usual XPS formalism are especially pronounced when the denominator in ratio (24) is small compared with unity. This is associated with the minima of the differential photoelectric cross section, pertaining to the emission directions perpendicular to the dominant direction of the electric-field vector oscillations. The physical reason of this is quite obvious: the electric field pushes a photoelectron out of an atom mainly in the directions parallel or antiparallel to the polarization vector. In the

next section some typical examples of the mean escape depth dependence on the major parameters are considered.

V. RESULTS AND DISCUSSION

In the dipole-approximation the initial angular distribution of photoelectrons ejected from atoms by polarized x rays is a function of the asymmetry parameter β and the three polarization parameters (p , γ , and η) and so is the mean escape depth. This results in a considerable variation in the mean escape depth as a function of emission angles and x-ray polarization. The main features of this dependence can be easily traced out by few examples. For the further analysis it is convenient to introduce the normalized mean escape depth

$$d = D/(\lambda_i \cos \alpha). \quad (33)$$

Note, that in the absence of elastic scattering the quantity d is always unity, $d=1$, in accordance with the usual XPS formalism.

In Figs. 3(a) and 3(b) the dependences of the mean escape depth d on the polarization degree p is shown for Al 2s ($\beta=2.00$) and Au 4s ($\beta=1.82$) photoelectrons emitted from a sample in the plane of incidence ($\phi=0$) in the directions perpendicular to that of photon propagation ($\alpha+\vartheta_\gamma=\pi/2$), correspondingly. In such a geometry only a minor influence of the asymmetry parameter β on the shape of the angular distribution is expected. The x rays are assumed to be linearly polarized along the y axis ($\gamma=0$, $\eta=90^\circ$) and their energy is put equal to the photon energy of Al $K\alpha$ radiation (1486.6 eV). The inelastic and the transport mean free paths calculated by the formula of Tanuma, Powell, and Penn²⁶ and that of Tilinin,²⁷ respectively, are equal to $\lambda_i=25.0$ Å and $\lambda_{tr}=227$ Å, in the case of aluminum and 10.4 and 17.2 Å for gold. Thus the ratio λ_i/λ_{tr} for aluminum is noticeably less than that of gold, which points to a much more strongly pronounced elastic-scattering effect for the gold target. From Fig. 3 it follows that the increase in the degree of polarization p leads to increasing the ratio $D/(\lambda_i \cos \alpha)$. The less the cosine of emission angle α is the more significant is the difference between the values of the mean escape depth obtained with and without taking into account elastic scattering of electrons. In the case of unpolarized radiation $p=0$ and the emission direction $\alpha=\pi/2-\vartheta_\gamma$ corresponds to a maximum of the initial angular distribution. As a result the normalized mean escape depth reaches its minimum value. Those minimum values, however, are significantly different for Al and Au targets. Thus, due to a small ratio $\lambda_i/\lambda_{tr}\sim 0.1$ the normalized mean escape depth for Al is close to unity for all emission angles considered, while for the Au target and near normal emission the quantity D differs from the product $\lambda_i \cos \alpha$ by almost 30%. The value $p=1.0$ pertains to a completely polarized photon beam with a polarization vector perpendicular to the photoelectron emission direction. In the latter case the angular distribution of emitted electrons has a minimum, while the mean escape depth reaches its maximum.

Figures 4(a) and 4(b) illustrate the azimuthal dependence of the mean escape depth for the linearly polarized radiation ($p=1.0$). The electric-field vector in the incident wave oscillates along the x axis. The samples are irradiated at the angle $\vartheta_\gamma=45^\circ$ and the photoelectron current is collected at

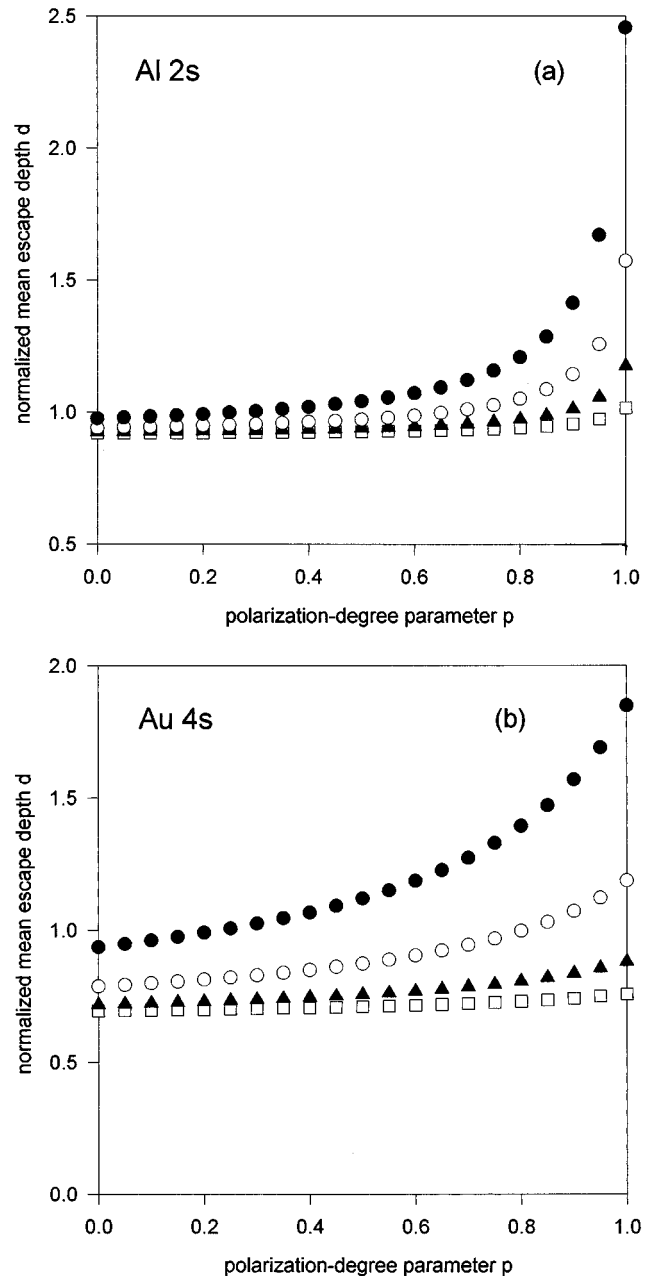


FIG. 3. Dependence of the normalized mean escape depth, $D/\lambda_i \cos \alpha$ on the polarization degree p for the Al 2s (a) and Au 4s (b) electrons escaping from a sample in the plane of incidence at different polar angles in the direction perpendicular to the propagation direction of x rays ($\alpha+\vartheta_\gamma=90^\circ$). Photons are polarized along the y axis ($\gamma=0$, $\eta=90^\circ$). Calculations were done using formulas (23) and (33). Open squares represent $\alpha=10^\circ$, black triangles= 50° , open circles= 70° , black circles= 80° .

the emission directions $\alpha=35$, 45 , 55 , 65 , and 75° which is close to a typical geometrical configuration in commercially available XPS setups. At relatively small emission angles $\alpha=0-45^\circ$ the escape depth has a maximum in the plane of incidence ($\phi=180^\circ$). This maximum splits in two off-plane maxima with increasing the polar angle α . The positions of these maxima are determined by the minima of the corresponding initial angular distribution [cf. formula (4)]. At the emission angle $\alpha=75^\circ$ the quantity D exceeds considerably

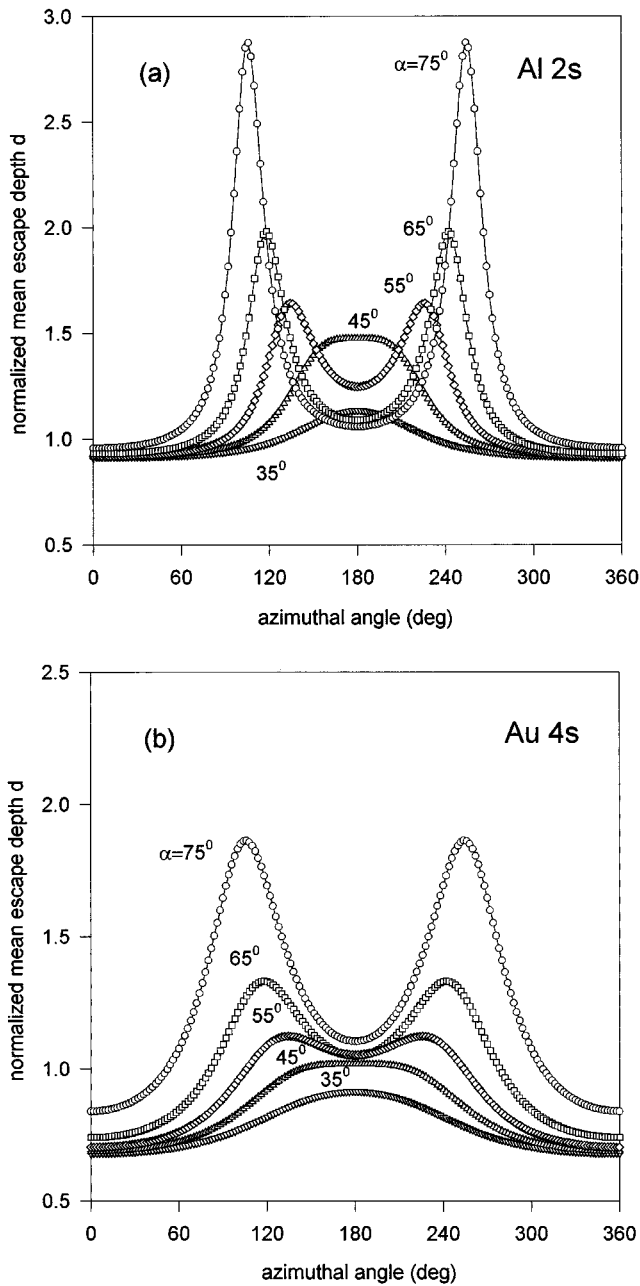


FIG. 4. Dependence of the normalized mean escape depth, $D/\lambda_i \cos\alpha$, on the azimuthal emission angle ϕ for Al 2s (a) and Au 4s (b) electrons ejected by a linearly polarized radiation ($p=1$, $\gamma=0$, $\eta=0$), and leaving a target at different polar emission angles α . The photon energy and angle of incidence are equal to 1486.5 eV and 45° , respectively. Triangles overturned represent $\alpha=35^\circ$, triangles=45°, diamonds=55°, squares=65°, and circles=75°.

the value predicted by the usual XPS formalism. Thus we have $D \sim 2.8\lambda_i \cos\alpha$ for aluminum and $D \sim 1.8\lambda_i \cos\alpha$ in the case of gold.

As a final example the mean escape depth dependence on the polarization type is illustrated in Figs. 5(a) and 5(b) for Al and Au targets. The angle of incidence of x rays is equal to 45° and a beam is completely polarized ($p=1.0$). The polarization vector is oriented along the y axis ($\gamma=90^\circ$). The photoelectrons are collected in the plane of incidence ($\phi=0$) in the emission directions $\alpha=40, 60, 70$, and 80° . The values

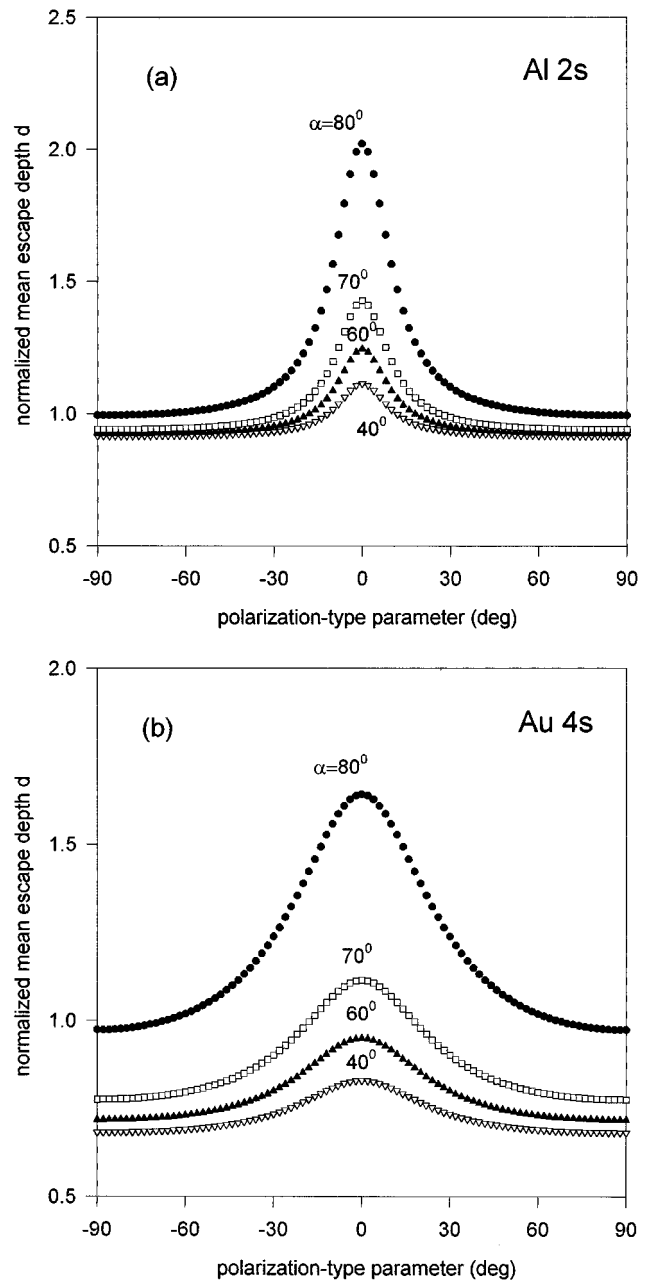


FIG. 5. Dependence of the normalized mean escape depth, $D/\lambda_i \cos\alpha$, on the type of polarization η for Al 2s (a) and Au 4s (b) photoelectrons ejected from a sample by a completely polarized x-ray beam incident on a sample at the angle $\vartheta_\gamma=0$ ($p=1$, $\gamma=90^\circ$). The photon energy is 1486.6 eV. Photoelectrons leave a solid at different polar emission angles in the plane of incidence. Open triangles overturned represent $\alpha=40^\circ$, black triangles=60°, open squares=70°, and black circles=80°. Calculations by formulas (23) and (33).

of the polarization type parameter $\eta=0$ and $\pm 90^\circ$ correspond to x rays linearly polarized along the y and x axes, respectively. In the case of the η parameter belonging to the intervals $(-90^\circ, 0)$ and $(0, +90^\circ)$ there are left ($\eta < 0$) and right ($\eta > 0$) elliptically polarized photon beams. For the chosen emission directions the relative number of recorded photoelectrons is minimal at $\eta=0$ as the plane of incidence is perpendicular to the electric-field vector. On the contrary the

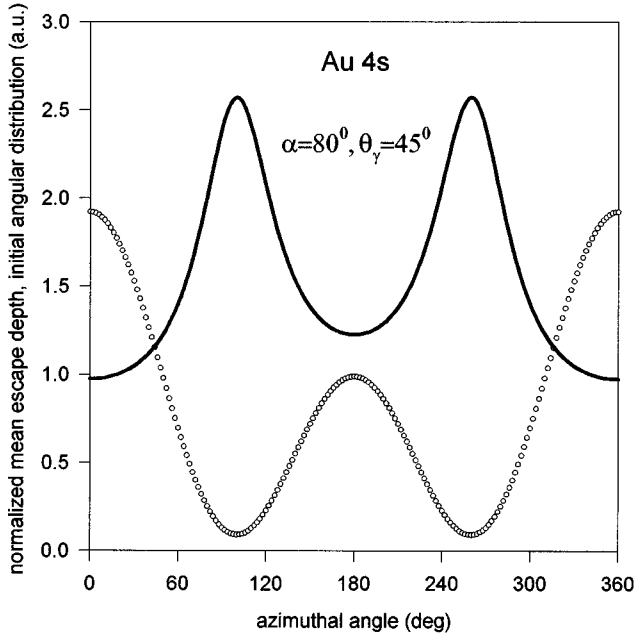


FIG. 6. The correlation between the normalized initial angular distribution (open circles) and the normalized mean escape depth dependence on the azimuthal emission angle (solid line) for Au 4s photoelectrons ejected by a linearly polarized radiation (1486.6 eV) incident on the target at the angle $\vartheta_\gamma=45^\circ$ ($\beta=1.82$, $p=1.0$, $\gamma=\eta=0$). Calculations by formulas (23), (33), (34), and (35). The photoelectron current is collected in the direction $\alpha=80^\circ$.

angular distribution reaches maximum values for $\eta=\pm 90^\circ$. Therefore, the normalized escape depth d is the smallest when the electric-field vector is parallel to the plane of incidence.

From the analysis of expression (23) and the examples presented above it follows that behavior of the mean escape depth is strongly correlated with the initial angular distribution of photoelectrons inside the target. This correlation is especially well seen in Fig. 6, where the quantity d along

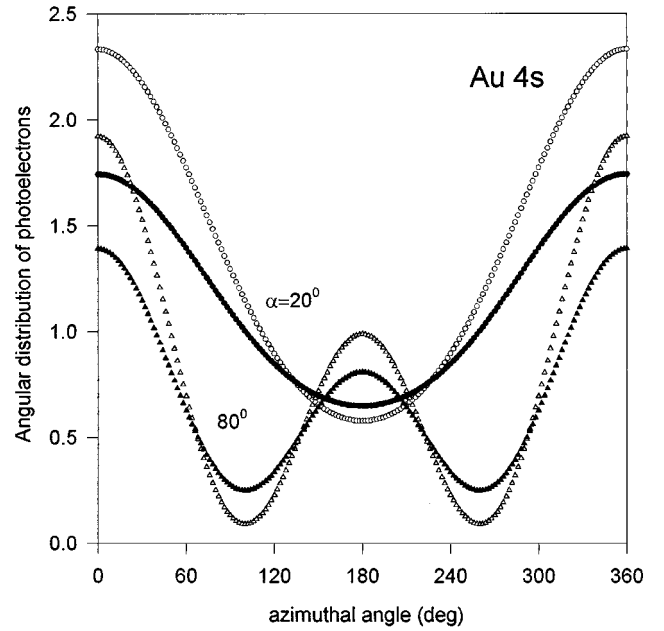


FIG. 7. The normalized distribution $Y=4\pi Y/y_0 \cos \alpha$ versus the azimuthal angle for 4s photoelectrons ejected from a gold target at different polar emission angles α by linearly polarized x rays ($p=1$, $\gamma=\eta=0$) incident at the angle $\vartheta_\gamma=45^\circ$. Black circles represent $\alpha=20^\circ$, black triangles= 80° [calculations by formulas (34) and (35)]. Open circles ($\alpha=20^\circ$) and triangles (80°) correspond to the straight-line approximation results (elastic scattering neglected).

with the initial distribution $f(\Theta, \Phi)$ of Au 4s photoelectrons is displayed as a function of the azimuthal angle. The linearly polarized ($\gamma=0$, $\eta=0$) x rays are incident on the surface at the angle $\vartheta_\gamma=45^\circ$, while photoelectrons escape from the target at the polar angle $\alpha=80^\circ$. The correlation effect can be understood upon examining closely the character of the angular distribution of photoelectrons leaving the sample. This distribution is proportional to the denominator of the ratio in the right-hand side of formula (22) and is given by the expression

$$Y(\alpha, \phi) = (y_0 \cos \alpha / 4\pi) \left\{ (1-\omega)^{-1/2} H(\cos \alpha, \omega) - \frac{\beta}{4} [3 \cos^2 \psi - 1 + 3S_1 \zeta_1(\alpha, \phi) + 3S_2 \zeta_2(\alpha, \phi)] \right. \\ \left. + \frac{\omega\beta}{16} [3\mu_\gamma^2 - 1 + 3S_1(1-\mu_\gamma^2)] \int_0^1 \frac{xH(x, \omega)H(\cos \alpha, \omega)(3x^2-1)dx}{x + \cos \alpha} \right\}. \quad (34)$$

Formula (34) follows immediately from expressions (4) and (12). The quantity $Y(\alpha, \phi) \sin \alpha d\alpha d\phi$ represents the total number of photoelectrons emitted by a unit area of the target surface in an infinitesimally small solid angle $\sin \alpha d\alpha d\phi$ along the direction (α, ϕ) . The result of the straight line approximation is obtained from formula (34) by setting $\lambda_{tr}=\infty$, $\omega=0$. In this case the differential photoelectron yield Y becomes proportional to the initial distribution of electrons inside the target. Analysis shows that, for typical values of the

ratio $\lambda_i/\lambda_{tr} \sim 0.2-0.5$, formula (34) approximately reproduces the initial angular distribution. However, distribution (34) is much smoother than that described by expression (4). Namely, the relative amount of electrons emitted from the solid in the directions of maxima is decreased, while the relative intensity of the photoelectron current in the directions of minima of the function $f(\Theta, \Phi)$ is increased. The smoothing effect of elastic collisions is illustrated by Fig. 7 where the normalized angular distribution

$$Y(\alpha, \phi) = 4\pi Y(y_0 \cos\alpha)^{-1} \quad (35)$$

is displayed versus the azimuthal angle ϕ for Au 4s photoelectrons ejected by x rays linearly polarized along the x axis ($p=1$, $\gamma=0$, $\eta=0$). The depletion of the photoelectron current in the most probable emission directions is caused by scattering of the electrons coming from deeper depths. These electrons are redistributed in such a way that they increase the yield in the directions at which initially only a small amount of particles move. As a result, the mean escape depth is effectively increased in those directions and vice versa.

It should be stressed that the anisotropical behavior of the mean escape depth is mostly pronounced for the intermediate values of the scattering parameter $\chi = \lambda_i/\lambda_{tr} \sim 1$. In the limiting case of large $\chi \gg 1$ intensive elastic scattering sweeps the escape probability of all anisotropic features. In the opposite limiting case of strong absorption $\chi \ll 1$ the angular dependence of the normalized mean escape depth is observed only in narrow solid angles in the vicinity of deep minima of the photoelectric cross section. For $\chi=0$ the quantity $d=1$ except for the emission directions corresponding to zeros of the initial angular distribution where the normalized escape depth is formally undefined.

The results obtained allow us to draw some general conclusions about the mean escape depth behavior of medium energy electrons in other physical problems involving initially anisotropical angular distributions. One of them is Auger and photoelectron diffraction.²⁸⁻³⁰ In crystalline targets a periodic arrangement of atoms gives rise to dynamical diffraction effects or coherent scattering. A coherent field of

signal Auger or photoelectrons later on gets through a relaxation process caused by incoherent elastic and inelastic scattering due to thermal displacements of atoms from their equilibrium positions^{31,32} and interaction with weakly bound electrons. Since the probability of coming back to a coherent state for an electron suffered diffuse scattering is small,^{33,34} the coherent field may be regarded as a source for incoherently scattered electrons. The angular distribution of coherently scattered electrons is noticeably anisotropic with peculiarities along the crystallographic axis directions. Thus, the mean escape depth of medium energy electrons is expected to be strongly anisotropic and to depend on the symmetry of a particular crystalline lattice. Recent numerical studies of photoemission from single crystals in the 1 keV energy range³⁵ supports this idea.

Another closely related phenomenon is spin-polarized photoemission from solids irradiated by soft x rays.³⁶⁻³⁸ The developed approach can be generalized for the case of a spin-resolved XPS theory. Preliminary results indicate that both the angular distribution and the mean escape depth of photoelectrons are strongly spin-dependent quantities. The latter should be taken into account when applying the inelastic background procedure to analyze the energy spectra of signal electrons in the vicinity of the characteristic peaks in spin-resolved photoemission experiments.^{39,40}

ACKNOWLEDGMENTS

The author would like to express his thanks to Dr. S. L. Dudarev and Dr. B. Schmiedeskampf for helpful discussions.

- ¹A. Jablonski and H. Ebel, *Surf. Interface Anal.* **11**, 627 (1988).
- ²1994 *Annual Book of Standards* (ASTM, Philadelphia, 1994), Vol. 3.06, p. 739.
- ³C. S. Fadley, R. J. Baird, W. Siekhaus, T. Novakov, and S. A. L. Bergstrom, *J. Electron Spectrosc. Relat. Phenom.* **4**, 93 (1974).
- ⁴I. S. Tilinin, A. Jablonski, and B. Lesiak-Orlowska, *Acta Phys. Pol.* **86**, 845 (1994).
- ⁵A. Jablonski, *Surf. Interface Anal.* **21**, 758 (1994).
- ⁶A. Jablonski, I. S. Tilinin, and C. J. Powell (unpublished).
- ⁷*Selected Experiments in Condensed Matter Physics with Synchrotron Radiation*, edited by W. Czaja (Birkhauser, Basel, 1991).
- ⁸F. J. Himpsel, *Acta Phys. Pol.* **86**, 771 (1994).
- ⁹C. Capasso, *Surf. Sci.* **287/288**, 1046 (1993).
- ¹⁰G. Margaritondo, *Acta Phys. Pol.* **86**, 705 (1994).
- ¹¹Keh-Ning Huang, *Phys. Rev. A* **22**, 223 (1980).
- ¹²A. R. Edmonds, *Angular Momentum in Quantum Mechanics* (Princeton University, Princeton, New Jersey, 1957).
- ¹³G. G. Stokes, *Trans. Cambridge Philos. Soc.* **9**, 399 (1852).
- ¹⁴U. Fano, *Rev. Mod. Phys.* **29**, 74 (1957).
- ¹⁵M. Born and E. Wolf, *Principles of Optics* (Pergamon, New York, 1959), p. 554.
- ¹⁶R. L. Reilman, A. Msezane, and S. T. Manson, *J. Electron Spectrosc. Relat. Phenom.* **8**, 289 (1976).
- ¹⁷I. S. Tilinin and W. S. M. Werner, *Phys. Rev. B* **46**, 13 739 (1992).
- ¹⁸I. S. Tilinin and W. S. M. Werner, *Mikrochim. Acta* **114/115**, 485 (1994).
- ¹⁹W. S. M. Werner and I. S. Tilinin, *Appl. Surf. Sci.* **70/71**, 29 (1993).
- ²⁰I. S. Tilinin and W. S. M. Werner, *Surf. Sci.* **290**, 119 (1993).
- ²¹I. S. Tilinin, A. Jablonski, and S. Tougaard, *Phys. Rev. B* **52**, 5935 (1995).
- ²²I. S. Tilinin, A. Jablonski, and B. Lesiak-Orlowska, *Acta Phys. Pol.* **86**, 853 (1994).
- ²³K. Case and P. Zweifel, *Linear Transport Theory* (Addison-Wesley, Reading, Massachusetts, 1967), p. 115.
- ²⁴I. S. Tilinin, A. Jablonski, and B. Lesiak-Orlowska, *Vacuum* **46**, 613 (1995).
- ²⁵S. Chandrasekhar, *Radiative Transfer* (Clarendon, Oxford, 1950).
- ²⁶S. Tanuma, C. J. Powell, and D. R. Penn, *Surf. Interface Anal.* **17**, 911 (1991).
- ²⁷I. S. Tilinin, *Zh. Eksp. Teor. Fiz.* **94**, 96 (1988) [*Sov. Phys. JETP* **67**, 1570 (1988)].
- ²⁸S. Y. Tong, H. C. Poon, and D. R. Snider, *Phys. Rev. B* **32**, 2096 (1985).
- ²⁹M.-L. Xu, J. J. Barton, and M. A. Van Hove, *Phys. Rev. B* **39**, 8275 (1989).
- ³⁰A. P. Kaduwela, D. J. Friedman, and C. S. Fadley, *J. Electron Spectrosc. Relat. Phenom.* **57**, 223 (1991).
- ³¹M. J. Whelan, *J. Appl. Phys.* **36**, 2099 (1965).
- ³²C. R. Hall and P. B. Hirsch, *Proc. R. Soc. London Ser. A* **286**, 158 (1965).
- ³³S. L. Dudarev and M. J. Whelan, *Surf. Sci.* **311**, L687 (1994).
- ³⁴W. S. M. Werner, I. S. Tilinin, and M. Hayek, *Phys. Rev. B* **50**, 4819 (1994).
- ³⁵S. D. Ruebush, R. X. Ynzunza, S. Thevuthasan, A. P. Kaduwela,

- M. A. Van Hove, and C. S. Fadley, *Surf. Sci.* **328**, 302 (1995).
- ³⁶J. Kirschner, *Polarized Electrons at Surfaces* (Springer, Berlin, 1985).
- ³⁷U. Heinzmann, *Phys. Scr. T* **17**, 77 (1987).
- ³⁸B. Schmiedeskampf, *Acta Phys. Pol. A* **86**, 675 (1994).
- ³⁹A. K. See and L. E. Klebanoff, *Phys. Rev. B* **51**, 7901 (1995).
- ⁴⁰Zhogle Xu, Y. Liu, P. D. Johnson, B. Itchkawitz, K. Randall, J. Feldhaus, and A. Brashaw, *Phys. Rev. B* **51**, 7909 (1995).